

K^+ nucleus reaction and total cross sections: New analysis of transmission experiments

E. Friedman,¹ A. Gal,¹ R. Weiss,² J. Aclander,² J. Alster,² I. Mardor,² Y. Mardor,² S. May-Tal Beck,² E. Piasezky,²
 A. I. Yavin,² S. Bart,³ R. E. Chrien,³ P. H. Pile,³ R. Sawafra,³ R. J. Sutter,³ M. Barakat,⁴ K. Johnston,⁴
 R. A. Krauss,⁵ H. Seyfarth,⁶ and R. L. Stearns⁷

¹*Racah Institute of Physics, The Hebrew University, Jerusalem 91904, Israel*

²*School of Physics, Raymond and Beverly Sackler Faculty of Exact Sciences, Tel-Aviv University, Tel Aviv 69978, Israel*

³*Department of Physics, Brookhaven National Laboratory, Upton, New York 11973*

⁴*Department of Physics, Louisiana Tech University, Ruston, Louisiana 71272*

⁵*Texas A & M University, College Station, Texas 77843*

⁶*Kernforschungsanlage Jülich G.m.b.H., D-52425 Jülich, Germany*

⁷*Vassar College, Poughkeepsie, New York 12601*

(Received 18 June 1996)

The attenuation cross sections measured in transmission experiments at the alternating-gradient synchrotron for K^+ on ${}^6\text{Li}$, C, Si, and Ca at $p_L = 488, 531, 656,$ and 714 MeV/ c are reanalyzed in order to derive total (σ_T) and reaction (σ_R) cross sections. The effect of plural (Molière) scattering is properly accounted for, leading to revised values of σ_T . We demonstrate the model dependence of these values, primarily due to the choice of K^+ nuclear optical potential used to generate the necessary Coulomb-nuclear and nuclear elastic corrections. Values of σ_R are also derived, for the first time, from the same data and exhibit a remarkable degree of model independence. The derived values of σ_T and σ_R exceed those calculated by the first-order $t\rho$ optical potential for C, Si, and Ca, but not for ${}^6\text{Li}$, particularly at 656 and 714 MeV/ c where the excess is 10–25%. Relative to ${}^6\text{Li}$, this excess is found to be nearly energy independent and its magnitude of 15–25% is not reproduced by any nuclear medium effect studied so far. [S0556-2813(97)01002-9]

PACS number(s): 25.80.Nv, 21.65.+f, 24.85.+p

I. INTRODUCTION

Total cross sections for the interaction of 500–700 MeV/ c K^+ with several nuclei were derived from transmission experiments performed at the alternating-gradient synchrotron in Brookhaven National Laboratory [1–4]. The high precision of these cross sections (about 1%) led to analyses of the data in terms of K^+ nucleus potentials, based on the expectation that the K^+ nucleus interaction is simply related to the KN interaction. In particular, in this energy range the KN interaction does not vary strongly with energy and together with the relative weakness of the interaction one expects that optical potentials close to the “ $t\rho$ ” approximation (see below) will be capable of describing the data. However, all such analyses showed disagreement between calculation and experiment at the level of 5–15%, which caused speculations about modifications in the nuclear medium of the KN interaction [5–8]. As an example for the difficulties encountered in such analysis we note that if one adjusts parameters of the potential, separately at each energy, to fit the total cross sections (σ_T) measured for ${}^6\text{Li}$, C, Si, and Ca, then the resulting potentials are vastly different from the “ $t\rho$ ” potentials used to derive these σ_T values. It is also noted that such potentials that fit these values of σ_T are questionable on account of predicting unacceptably small values for the reaction cross section (σ_R). This complicated state of affairs motivated the present study.

In the present work we reexamine the derivation of integral cross sections for K^+ nucleus interaction from the previously measured attenuation cross sections for K^+ on ${}^6\text{Li}$, C, Si, and Ca at 488, 531, 656 and 714 MeV/ c . It is demon-

strated in Sec. II that σ_R values extracted from such measurements are likely to be less model dependent than σ_T values are. Revised values for σ_T are presented in Sec. III where the effects of plural scattering are now included together with various other effects such as the dependence on the particular nuclear density used in the optical model or the way the various KN partial waves are handled. Results for σ_R are presented for the first time. In Sec. IV we study the effect of constraining the analysis with differential cross sections for the elastic scattering of K^+ on ${}^6\text{Li}$ and C at 715 MeV/ c that have become available very recently. We also discuss the model dependence of the various results, their dependence on the particular form of wave equation and potential used in the analysis, and whether or not the new data may indicate medium effects in the K^+ nucleus interaction.

II. TRANSMISSION MEASUREMENTS ON NUCLEI

The derivation of meson-nucleus integral cross sections from measurements of the attenuation of a beam as a function of solid angle of a detector is an old and established technique [9,10]. Defining the reaction cross section σ_R as the integral cross section for removal of particles from the elastic channel, the attenuation cross section for removal of particles from a detector subtending a solid angle Ω at the target is

$$\sigma_{\text{att}}(\Omega) = \sigma_R + \int_{\Omega}^{4\pi} \left(\frac{d\sigma}{d\Omega} \right)_{\text{el}} d\Omega - \int_0^{\Omega} \left(\frac{d\sigma}{d\Omega} \right)_{\text{ne}} d\Omega \quad (1)$$

where the second term on the r.h.s. represents elastically scattered particles that miss the detector and the third term

represents nonelastic reaction products that are detected. By subtracting the second (elastic) term from the experimentally determined attenuation cross section one defines $\sigma_R(\Omega)$ as follows

$$\sigma_R(\Omega) = \sigma_{\text{att}}(\Omega) - \int_{\Omega}^{4\pi} \left(\frac{d\sigma}{d\Omega} \right)_{\text{el}} d\Omega. \quad (2)$$

The value of σ_R is obtained by extrapolating this $\sigma_R(\Omega)$ to $\Omega=0$ because the third (nonelastic) term on the rhs of Eq. (1) vanishes for $\Omega=0$. It is therefore clear that the value of σ_R obtained from the extrapolation to $\Omega=0$ depends on values of cross sections for elastic scattering to angles larger than Ω . When these cross sections are known from experiment the values of $\sigma_R(\Omega)$ are unambiguously given by Eq. (2). However, in the case that these cross sections are not available experimentally, it is necessary to use an optical potential to calculate the corrections due to elastic scattering, thus creating a possible dependence between the extracted σ_R and the optical potential. This procedure naturally raises the question of consistency between the assumed potential and the resulting σ_R . When the analysis of transmission experiments is aimed at the extraction of a total cross section, a total nuclear elastic cross section is added to the quantities being extrapolated,

$$\sigma_T(\Omega) = \sigma_R(\Omega) + \int_0^{4\pi} |f_N|^2 d\Omega \quad (3)$$

where f_N is the nuclear elastic scattering amplitude. This additional term is never available experimentally for charged particles, thus making σ_T for charged particles always dependent on some optical model calculations.

It is convenient to write the differential cross section for elastic scattering in terms of a sum of nuclear and Coulomb amplitudes:

$$\left(\frac{d\sigma}{d\Omega} \right)_{\text{el}} = |f_N + f_C|^2 = |f_N|^2 + |f_C|^2 + 2\text{Re}[f_N f_C^*]. \quad (4)$$

The dependence of the elastic correction on the optical potential then enters via the nuclear term ($|f_N|^2$) and Coulomb-nuclear interference term ($2\text{Re}[f_N f_C^*]$). Substituting $\sigma_R(\Omega)$ from (2) and using the f_N and f_C amplitudes, one obtains

$$\begin{aligned} \sigma_T(\Omega) &= \sigma_{\text{att}}(\Omega) - \int_{\Omega}^{4\pi} |f_N + f_C|^2 d\Omega + \int_0^{4\pi} |f_N|^2 d\Omega \\ &= \sigma_{\text{att}}(\Omega) + \int_0^{\Omega} |f_N|^2 d\Omega - \int_{\Omega}^{4\pi} |f_C|^2 d\Omega \\ &\quad - 2 \int_{\Omega}^{4\pi} \text{Re}[f_N f_C^*] d\Omega. \end{aligned} \quad (5)$$

It is clear that an optical potential is needed to obtain $\sigma_T(\Omega)$ and the question of consistency will always arise.

In Fig. 1 we demonstrate the differences between σ_R and σ_T in terms of the optical-model input that goes into the analysis of transmission measurements. The example shown is for 714 MeV/c K^+ on carbon where we plot the experimental $\sigma_{\text{att}}(\Omega)$ and the calculated $\sigma_R(\Omega)$ [Eq. (2)] and

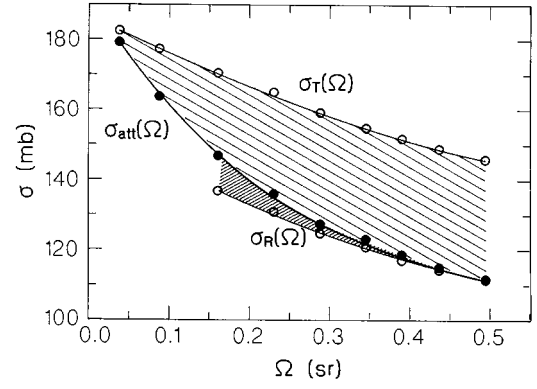


FIG. 1. Experimental attenuation cross sections (solid dots, middle curve), calculated total cross sections (open circles, upper curve), and calculated reaction cross sections (open circles, lower curve) for carbon at 714 MeV/c as function of the solid angle of the detector. The shaded areas indicate the theoretical input into $\sigma_T(\Omega)$ and $\sigma_R(\Omega)$. Corrections due to kaon decay are not included.

$\sigma_T(\Omega)$ [Eq. (5)]. A “ $t\rho$ ” potential (see below) is used in the optical model calculations. It is clearly seen that as Ω increases the calculated input into $\sigma_T(\Omega)$ increases and reaches a fairly large fraction of the measured $\sigma_{\text{att}}(\Omega)$. In contrast, the calculated input into $\sigma_R(\Omega)$ vanishes as Ω increases. Although the extrapolation to $\Omega=0$ should become more accurate as more points are included for small angles, these points involve increasingly large calculated corrections, thus making the extrapolated value more dependent on the optical potential. Figure 1 thus suggests that when the model dependence of the extrapolated cross sections is being considered, then σ_R is indeed the more reliable quantity that may be derived from transmission measurements.

Uncertainties in the extrapolation of $\sigma_T(\Omega)$ to $\Omega=0$ were discussed previously leading to conflicting conclusions. Arima and Masutani [11] showed that except for light nuclei errors of 10% can arise in the process of extrapolation whereas Kaufmann and Gibbs [12] showed that varying the nuclear elastic term in Eq. (5) by $\pm 20\%$ leads to the same extrapolated values. This latter test is irrelevant as it merely modifies the slope of a term that in any case extrapolates to zero. A realistic test would be to vary the optical potential by imposing some physical constraints such as fits to elastic scattering data. This will be done in Sec. IV of this paper.

The need to avoid very small angles in transmission measurements on nuclei had been known long ago [9,10]. In the present analysis we have used only the largest seven solid angles ($\Omega \geq 0.166$ sr) to obtain reaction cross sections whereas at least 8 angles, and in most cases all 9 angles were used to obtain total cross sections. In view of Eq. (3) one must not take the same experimental points in the two analyses, otherwise the extracted σ_T and σ_R values will differ by just the total nuclear elastic cross section implied by the optical potential used in the analysis.

III. ANALYSIS AND RESULTS

A. Optical potentials

As discussed in the previous section an optical potential is needed in order to obtain the correction terms when σ_T is to

TABLE I. Examples for corrections due to plural scattering. Uncertainties are due to the statistics of the Monte Carlo calculation.

Target momentum (MeV/c)	C 488				Ca 714			
Solid angle (sr)	0.0422	0.0890	0.1661	0.2321	0.0422	0.0890	0.1661	0.2321
$\Delta\sigma$ (mb)	5.8 ± 0.4	2.6 ± 0.3	1.4 ± 0.2	0.85 ± 0.15	22.8 ± 1.4	9.8 ± 0.9	5.3 ± 0.7	3.7 ± 0.5

be derived from experiment. The potential is needed also for deriving σ_R when the integral of the elastic scattering differential cross section [Eq. (2)] cannot be evaluated directly from experimental results, which is the case in the present work. Because of the long mean free path of K^+ in nuclei in the present energy range, nuclei are expected to be fairly transparent to K^+ and as a result the K^+ -nucleus optical potential may be simply related to the KN forward scattering amplitude $f_{c.m.}(0)$ and nuclear density $\rho(r)$ as follows:

$$2\varepsilon_{c.m.}^{(A)}V_{opt}(r) = -4\pi F_k f_{c.m.}(0)\rho(r), \quad (6)$$

where $\varepsilon_{c.m.}^{(A)}$ is the kaon total energy in the kaon-nucleus c.m. system and F_k is a kinematical factor (discussed below) resulting from the transformation of amplitudes between the KN and the K^+ -nucleus c.m. systems. The nuclear density distribution $\rho(r)$ is normalized to A , the number of nucleons in the target nucleus. This “ $t\rho$ ” optical potential [13] is then included in a Klein-Gordon equation for the meson-nuclear wave function, as described earlier in analyses of reaction cross sections of pions on nuclei in the 1 GeV energy range [10]. The form of the meson-nuclear relativistic wave equation is not unambiguous and we return to this point in Sec. IV.

The optical potential given by Eq. (6) may be used to calculate the correction terms needed to extract σ_T and σ_R from the measured attenuation cross sections. The KN amplitude $f_{c.m.}(0)$ was taken from KN phase shifts as given by SAID [14]. In the present energy range the contribution of partial waves higher than s in the kaon-nucleon interaction cannot be neglected. We have adopted two models for handling p and higher partial waves. In the first, the contributions of *all* higher partial waves were lumped together with the s -wave term to produce the (effective scattering length) complex parameter b_0 in the following potential

$$2\varepsilon_{c.m.}^{(A)}V_{opt}(r) = -4\pi F_k b_0 \rho(r). \quad (7)$$

In the second model the p -wave term was retained explicitly in the potential which then became a Kisslinger-like potential with a gradient term

$$2\varepsilon_{c.m.}^{(A)}V_{opt}(r) = -4\pi F_k [\tilde{b}_0 \rho(r) - G_k c_0 \vec{\nabla} \rho(r) \cdot \vec{\nabla}], \quad (8)$$

where G_k is another kinematical factor to be discussed below. The contributions by d and higher partial waves were included in \tilde{b}_0 . It will be shown below that the differences between the results obtained from the two models are exceedingly small.

Another ingredient of the potential are the nuclear densities $\rho(r)$. Two models were used for these: (i) a macroscopic (MAC) model where proton and neutron densities are given either by a two-parameter Fermi distribution (for Si and Ca) or a modified harmonic oscillator density distribution (for ${}^6\text{Li}$ and C). The parameters of these distributions were obtained by folding in the charge distribution of the proton to obtain a best fit to the corresponding charge distribution of the target nucleus [15]; (ii) a single particle (SP) model where the proton (ρ_p) and neutron (ρ_n) distributions in the nucleus are obtained by filling in single particle levels in Woods-Saxon potentials, requiring that the binding energy of the least bound particle agrees with experiment and that, after folding ρ_p with the charge distribution of the proton, the charge distribution of the target nucleus is reproduced. For ρ_n in the present self-conjugate nuclei we assumed the same parameters as for protons in the MAC model, or the same potential radii in the SP model. The SP densities are expected to be better approximations outside of the nuclear surface because they are based on the correct binding energies. By using two models for the nuclear densities we could therefore check the effects of ρ on the results.

B. Plural scattering

Multiple Coulomb scattering of beam particles by electrons in the target usually does not affect transmission measurements if the solid angles are not too small. However, in the case of multiple scattering with one large angle (nuclear scattering, usually referred to as Molière or plural scattering [16], there could be loss of particles out of the detector. This effect was not included in the previous analysis of this experiment but it was found not to be negligible at the smallest angles, particularly at the lowest energy and for the heaviest target. Corrections to the attenuation cross sections were calculated using the MLR subroutine [17] and typical results are shown in Table I. Some of these corrections are larger than the previously reported errors. In the present analysis these corrections were applied at all angles and energies for the four targets.

C. Results

The experimental attenuation cross sections were corrected for plural scattering and the terms calculated from the $t\rho$ potential in the form of Eq. (8) were added to obtain $\sigma_R(\Omega)$ [Eq. (2)] and $\sigma_T(\Omega)$ [Eq. (5)]. When the potential in the form of Eq. (7) was used, the extrapolated values differed by usually less than 1%. The last seven angles only were used for σ_R but all nine angles were used for σ_T at the two

TABLE II. Reaction and total cross sections (in mb) for K^+ interaction with various nuclei. Uncertainties due to the use of optical potentials are not included (see text).

Momentum (MeV/c)	Reaction				Total				
	${}^6\text{Li}$	C	Si	Ca	${}^6\text{Li}$	C	Si	Ca	D
488	65.0 ± 1.3	120.4 ± 2.3	265.5 ± 5.1	349.9 ± 7.7	76.6 ± 1.1	162.4 ± 1.9	366.5 ± 4.8	494.6 ± 7.7	25.33 ± 0.61
531	69.8 ± 0.8	129.3 ± 1.4	280.4 ± 3.4	367.1 ± 4.5	78.8 ± 0.7	166.6 ± 1.3	374.8 ± 3.3	500.2 ± 4.4	27.15 ± 0.32
656	75.6 ± 1.1	141.8 ± 1.5	306.1 ± 3.4	401.1 ± 5.0	84.3 ± 0.7	174.9 ± 0.8	396.1 ± 2.7	531.9 ± 4.2	28.15 ± 0.24
714	79.3 ± 1.2	149.3 ± 1.5	317.5 ± 3.6	412.9 ± 5.5	87.0 ± 0.6	175.6 ± 0.9	396.5 ± 2.3	528.4 ± 2.8	28.65 ± 0.20

higher momenta. At the two lower momenta only eight angles were used for σ_T because no satisfactory fit could be obtained to $\sigma_T(\Omega)$ vs Ω when the smallest angle was included. That fit, and also the fit to $\sigma_R(\Omega)$, was either a linear or a quadratic fit, as the case required, in order to achieve a χ^2 per degree of freedom close to or smaller than one. The extrapolated values were then corrected for kaon decays as in the previous analysis [4]. The procedure was repeated with both macroscopic and single particle models for the nuclear densities $\rho(r)$ and the extrapolated values of σ_R and σ_T were found to differ by no more than 1%. In the final values presented in Table II this uncertainty due to the model has been added quadratically to the other errors. The errors quoted do not include uncertainties due to the use of optical potentials. These additional errors are discussed in Sec. IV B.

The total cross sections for K^+ interacting with deuterium were obtained earlier from the differences between CD_2 and C targets and between LiD and Li targets. The effect of plural scattering corrections on these differences was found to be negligibly small. Therefore the published [4] cross sections for $K^+\text{D}$ remain unchanged. These σ_T values are included for completeness in Table II.

IV. DISCUSSION

A. Wave equations and potentials

Here we use the same Klein-Gordon (KG) equation in the projectile-nucleus center-of-mass (c.m.) system as done [Eq. (5.14) of Ref. [10]] previously for deriving pion-nucleus reaction cross sections in the 1 GeV region:

$$[\nabla^2 + k^2 - (2\varepsilon_{\text{c.m.}}^{(A)}V - V_c^2)]\psi = 0 \quad (\hbar = c = 1). \quad (9)$$

The quantities k and $\varepsilon_{\text{c.m.}}^{(A)}$ are the projectile wave number and energy respectively in the c.m. system, satisfying $(k^2 + m^2)^{1/2} = \varepsilon_{\text{c.m.}}^{(A)}$, where m is the projectile mass. V_c is the Coulomb potential due to the charge distribution of the nucleus, and $V = V_c + V_{\text{opt}}$. For a finite-mass target nucleus, and discarding V_c^2 , Eq. (9) does not reduce to the nonrelativistic Schrödinger equation for $k \rightarrow 0$, since then $\varepsilon_{\text{c.m.}}^{(A)} \rightarrow m$ instead of $\mu^{(A)}$ where the latter is the projectile-nucleus re-

duced mass. This distinction between m and $\mu^{(A)}$ of course disappears in the limit of an infinitely heavy target nucleus.

The first-order optical potential is given in the laboratory (lab) system by $V_{\text{opt}} = t\rho$, where t is the lab projectile-nucleon forward t matrix and ρ is the target nucleus matter density distribution normalized to A . Transforming to the projectile-nucleus c.m. system (Sec. 3.3 of Ref. [13]) and expressing t via the c.m. projectile-nucleon forward scattering amplitude $f(0^\circ)$, one arrives at the form given by Eq. (7) above, with $b_0 = f(0^\circ)$ and

$$F_k = \frac{M'}{M} A \sqrt{\frac{s}{E_{\text{c.m.}}^{(A)}}}, \quad (10)$$

where M is the free nucleon mass, AM' is the mass of the target nucleus, \sqrt{s} is the total projectile-nucleon energy in their c.m. system and $E_{\text{c.m.}}^{(A)}$ is the target nucleus energy in the projectile-nucleus c.m. system.

In the energy range of the present work the contribution of p waves to the K^+ -nucleon interaction is significant. This raises the question of whether or not to include p waves explicitly in the K^+ -nucleus potential. If the p -wave term $c_0 \vec{k}_{\text{c.m.}} \cdot \vec{k}'_{\text{c.m.}}$ of the projectile-nucleon c.m. scattering amplitude $f(\theta)$ is singled out, then $\vec{k}_{\text{c.m.}}$ is transformed (in the forward direction) to the projectile-nucleus c.m. momentum \vec{k} , thus giving rise to a gradient term as follows:

$$\vec{k}_{\text{c.m.}} = G_k^{1/2} \vec{k} \rightarrow G_k^{1/2} (-i\vec{\nabla}), \quad (11)$$

with

$$G_k^{1/2} = \frac{M}{M'} \frac{\sqrt{s^{(A)}}}{A\sqrt{s}}, \quad (12)$$

where $\sqrt{s^{(A)}}$ is the total projectile-nucleus energy in their c.m. system. This leads to the form given by Eq. (8) above, where

$$\tilde{b}_0 = f(0^\circ) - c_0 k_{\text{c.m.}}^2. \quad (13)$$

TABLE III. Parameter values for the optical potentials. Momenta are in MeV/c, b_0 , and \tilde{b}_0 in fm, c_0 in fm³.

Momentum	Potential Eq. (7)		Potential Eq. (8)			
	Re b_0	Im b_0	Re \tilde{b}_0	Im \tilde{b}_0	Re c_0	Im c_0
488	-0.178	0.153	-0.253	0.104	0.0337	0.0222
531	-0.172	0.170	-0.251	0.109	0.0309	0.0238
656	-0.165	0.213	-0.245	0.124	0.0221	0.0244
714	-0.161	0.228	-0.241	0.130	0.0191	0.0234

Table III summarizes the values of the optical potential parameters for the four energies of the present work. We stress that the contributions due to d and higher partial waves are included in both b_0 and \tilde{b}_0 .

Calculations were made with both forms of potentials. The values of σ_R and σ_T predicted by the potentials were found to be the same to within 1% regardless of the potential used. The same is true for the extrapolated values of σ_R and σ_T that in most cases differ by much less than 1% when the form of the potential is changed from Eq. (8) to Eq. (7), using the corresponding values from Table III. This result is not surprising in view of the long mean-free path of K^+ in nuclei in this energy range which should make the surface gradient terms equivalent to the corresponding volume terms. This is in contrast to the situation with low-energy pions.

We have also checked the sensitivity of our extrapolation and calculation procedures to the type of relativistic wave equation used by considering the Goldberger and Watson (GW) equation (Sec. 6.8 of Ref. [13])

$$\left\{ \nabla^2 + k^2 - \frac{AM'}{\sqrt{s^{(A)}}} [2(\sqrt{s^{(A)}} - AM')V - V_c^2] \right\} \psi = 0. \quad (14)$$

This equation reduces to the nonrelativistic Schrödinger equation for $k \rightarrow 0$ upon discarding the V_c^2 term. In the limit of an infinitely heavy target nucleus, Eq. (14) coincides with Eq. (9). Using Eq. (14) instead of Eq. (9) for extrapolating the curves $\sigma_T(\Omega)$ and $\sigma_R(\Omega)$ of Fig. 1 leads at 714 MeV/c to σ_T and σ_R derived values which differ from those in Table II by less than 1% for C and less than 0.2% for Ca. The cross-section values calculated by using Eq. (14) are *lower* by about 4% for C and by about 1% for Ca than those calculated by using Eq. (9).

B. Constraints due to elastic scattering

As discussed in Sec. II, σ_R can be evaluated from transmission measurements without the need to assume any optical potential if differential cross sections for elastic scattering are available from experiment such that the integral in Eq. (2) may be calculated for the required solid angles Ω . Differential cross sections have become recently available for the elastic scattering of 715 MeV/c K^+ by ${}^6\text{Li}$ and C [18], so one may adjust optical potential parameters to fit the data and then use the same parameters to analyze the transmission measurements on all four nuclei at 714 MeV/c. In this way the analysis of the transmission measurements becomes constrained by the elastic-scattering results. Similar data unfortunately do not exist at the other energies of interest here.

In the spirit of the present approach where the interaction of K^+ with all four nuclei is described at a given energy by a common optical potential (i.e., common b_0 , \tilde{b}_0 , and c_0 parameters), we tried to fit the elastic-scattering data for ${}^6\text{Li}$ and C by a common potential. Using the parameters of Table III or even adjusting the values of b_0 , or \tilde{b}_0 and c_0 , resulted in rather poor fits, particularly at larger angles. Trying to improve the fits by folding a KN interaction form factor into the nuclear density helped only marginally, but at the cost of causing the calculated σ_T and σ_R to decrease far below the anticipated values. As most of the contribution to the integral in Eq. (2) comes from small angles, we have repeated the fits to the elastic data, retaining only the five forward angles for each of the targets (covering Ω up to 0.7 sr). The fits were still quite poor and we have therefore introduced a phenomenological density-dependent (DD) modification of the interaction of the same form that was successful in analyzing hadronic atoms [19] in an attempt to obtain acceptable fits to the elastic-scattering data without losing completely the ability to get agreement with the measured σ_R and σ_T values. It consists of replacing \tilde{b}_0 by a DD term

$$\tilde{b}_0 \rightarrow \tilde{b}_0 + B_0 \left[\frac{\rho(r)}{\rho(0)} \right]^\alpha \quad (15)$$

and adjusting B_0 and α to fit the data. Reasonably good fits to the elastic-scattering data could thus be obtained, with the \tilde{b}_0 values of Table III and empirical values for B_0 (complex) and α . The same values of B_0 and α were then used in the optical model input to the analysis of the transmission experiments at 714 MeV/c. The results of this constrained analysis are shown in Table IV, where the corresponding $t\rho$ results from Table II are also given for comparison.

It is noted that the extrapolated values of σ_T are quite

TABLE IV. Reaction and total cross sections (in mb) at 714 MeV/c for different optical potentials used in the extrapolations. Only the statistical errors of Table II are included.

Potential	Reaction				Total			
	${}^6\text{Li}$	C	Si	Ca	${}^6\text{Li}$	C	Si	Ca
DD	80.0	149.2	317.7	413.4	91.2	192.1	433.9	589.6
	± 1.2	± 1.5	± 3.6	± 5.5	± 0.6	± 0.9	± 2.3	± 2.8
$t\rho$	79.3	149.3	317.5	412.9	87.0	175.6	396.5	528.4
	± 1.2	± 1.5	± 3.6	± 5.5	± 0.6	± 0.9	± 2.3	± 2.8

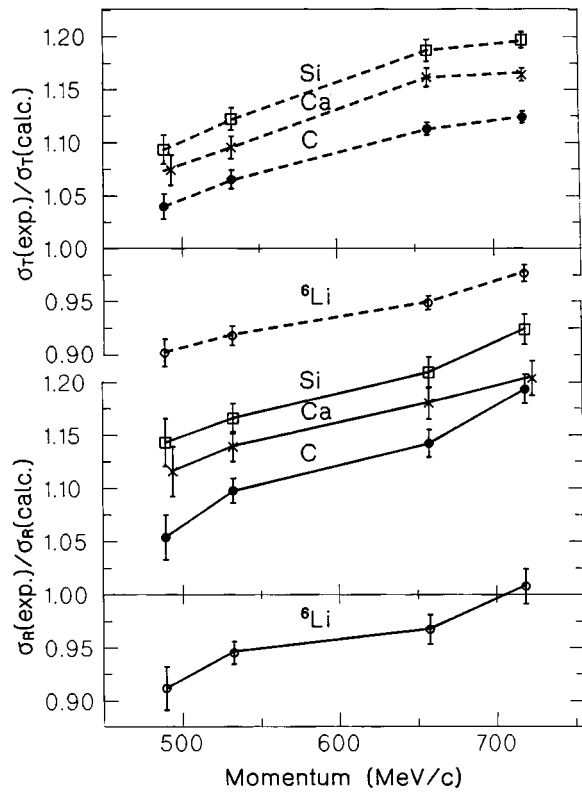


FIG. 2. Ratios between experimental and calculated cross sections based on a $t\rho$ potential: total cross sections — dashed curves (upper part); reaction cross sections — solid curves (lower part). The curves serve merely to guide the eye.

different in the two cases, by up to 10%. Both optical potentials are acceptable in this context: that of Table II is the $t\rho$ potential which is expected to provide a good starting point for a projectile with such a relatively long nuclear mean-free path as the K^+ . The DD potential of Table IV is an *ad hoc* solution devised to be constrained by elastic-scattering data, and is used here to demonstrate the model dependence of the extrapolated cross sections. The differences in values of σ_T are 10–20 times larger than the quoted errors [4], thus making the values of σ_T derived from transmission measurements strongly model dependent. This is in agreement with Arima and Masutani [11] and with the discussion of Sec. II. It therefore seems reasonable to assign additional errors of $\pm 5\%$ due to uncertainties in the optical potentials used in the analysis. In sharp contrast to this conclusion the values of σ_R for the DD potential are very close to the corresponding values for the $t\rho$ potential, the differences being considerably smaller than the quoted errors. Note that the relative statistical errors for the reaction cross sections are larger than the relative statistical errors for the total cross sections and, judging by the results of Table IV, they seem to cover also the uncertainties due to the use of optical potentials. Reaction cross sections therefore emerge as the less model-dependent quantities that can be derived from transmission measurements.

C. The problem of self consistency

The derivation of σ_R and σ_T from transmission measurements involves the use of an optical potential. The potential

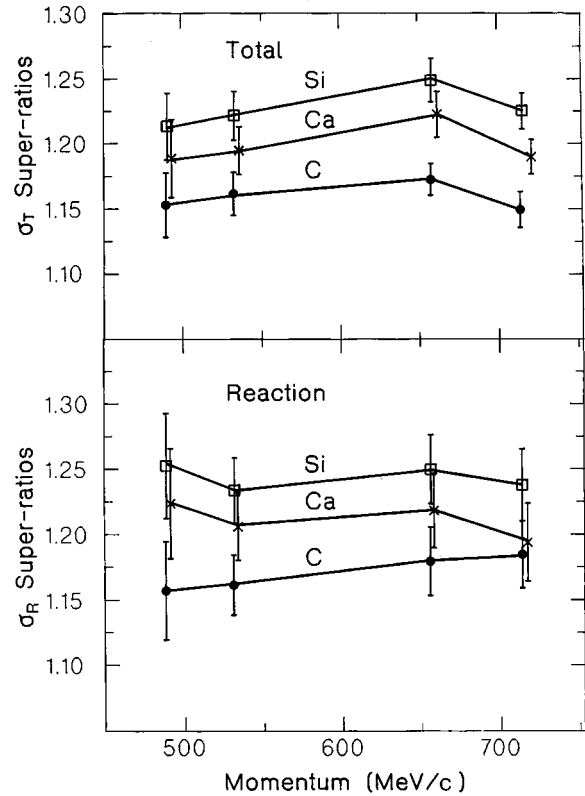


FIG. 3. Super ratios relative to ${}^6\text{Li}$: experimental cross sections relative to calculated values using a $t\rho$ potential, divided by the corresponding ratios for ${}^6\text{Li}$.

predicts reaction and total cross sections and an obvious question is whether σ_R and σ_T derived from experiment agree, or at least are consistent, with those predicted values. An alternative way to pose this question is the following: if an empirical optical potential is fitted to the σ_R and σ_T values derived from experiment, for all target nuclei, will the same values be obtained if the transmission measurements are reanalyzed using this empirical potential? The present answer to these questions is, unfortunately, negative. As mentioned in the Introduction, the inconsistency was observed with the values of σ_T published previously, where potentials fitted to the σ_T values departed strongly from those used in the analysis. Repeating such fits to the new results summarized in Table II, reasonably good fits are possible only with a DD potential [Eq. (15)] which differs from the $t\rho$ potential of Table III such that no consistency is possible. We note that in contrast to the repulsive $t\rho$ potential the DD potential is attractive in the interior of the nucleus which is hard to accept for K^+ in this energy range. If we fit only the σ_R values, which are the more reliable quantities derived from experiments, then the predicted values for σ_T become unreasonably large, e.g., 50–100% larger than those of Table II, which is far beyond any expected model dependence. When fits are made only to the σ_T values, then the predicted σ_R values turn out too small. This holds true for both $t\rho$ and DD potentials. The DD potentials that are constrained by the elastic-scattering data for ${}^6\text{Li}$ and C also predict too large value for the difference $\sigma_T - \sigma_R$. Note that such inconsistency is not observed with pion-nucleus potentials below 100 MeV [20].

D. Effects of the nuclear medium

There are several ways of inferring from the present results possible effects of the nuclear medium on the KN interaction. In the following we use the results summarized in Table II: for σ_R these are essentially model independent and for σ_T they are based on employing corrections due to the $t\rho$ potential which is expected to be an adequate starting point. One must bear in mind, however, that this potential is in conflict with the constrained analysis of Sec. II B.

It is useful to first note that the experimental values of σ_T/A for ${}^6\text{Li}$ are in agreement with the corresponding values for deuterium [4], as expected when the interaction is dominated by single scattering. This result also suggests that effects due to the nuclear medium are not important in the very light and loosely bound ${}^6\text{Li}$ nucleus. Values of σ_T/A for other nuclei cannot be directly compared to the deuterium values because for heavier nuclei effects due to multiple scattering are not negligible. For that reason it is useful then to compare experimental cross sections with those calculated by using the $t\rho$ optical potential throughout. Although the use of an optical potential for as light a nucleus as ${}^6\text{Li}$ might be questionable, we note that $1/A$ kinematical terms are properly included through the F_k and G_k coefficients [Eqs. (7) and (8)]. Figure 2 shows the ratios between experimental and calculated total and reaction cross sections for the four nuclei studied in the present work. For both types of cross sections these ratio plots display remarkably similar behavior, with ${}^6\text{Li}$ being very much lower than the other three and all exhibiting the same dependence on beam energy. Focusing on the dependence on the nuclear medium, Fig. 3 shows super ratios, i.e., the above ratios divided by the corresponding ratios for ${}^6\text{Li}$, where nuclear medium effects are presumably negligibly small. In this way the energy dependence of the above ratios is removed and one is left with a clear dependence on the nucleus involved. These results show that the cross sections for C, Si, and Ca are 15–25% larger than expected and therefore *could* indicate an enhancement of the KN interaction in nuclei compared to the interaction with free nucleons. We note that the bulk nuclear density of Si is larger than that of Ca or C and indeed the enhancement in the case of Si is more pronounced. The observed differences between Ca and C could result from carbon still being a relatively small nucleus where the full extent of the enhancement is not realized. It is interesting to note that the σ_R ratios and super ratios which are presented for the first time are very similar to the corresponding σ_T ratios and super ratios.

V. SUMMARY

In the present work we have reanalyzed the transmission measurements that had been used already to derive total cross sections σ_T for 488 to 714 MeV/c K^+ on several nuclei [4]. In the present, new analysis we have included corrections due to plural scattering which caused changes in the results. In addition we have extracted, for the first time, reaction cross sections σ_R for the same nuclei. By carefully studying the model dependence of the results, mostly due to the inevitable optical-model input into the analysis, we showed that σ_R values are essentially model independent whereas σ_T values depend on the model. When using a $t\rho$ potential in the analysis it is found that the analysis process

is not self-consistent and the situation does not improve when constraining the analysis with some recent data for elastic scattering [18]. Data that will be most useful in sorting out these difficulties are angular distributions for elastic scattering of K^+ for all four targets at all four momenta, that will make it possible to evaluate the elastic correction to σ_R [Eq. (2)] without the need to employ any potential. In addition, small angle angular distributions will hopefully provide unambiguous optical potentials.

Accepting the $t\rho$ potential, we obtained $\sigma(\text{expt})/\sigma(\text{calc})$ ratio values for σ_T that show both energy dependence and dependence on the target nucleus which are very similar to those for the less model-dependent σ_R . Super ratios formed relative to ${}^6\text{Li}$ are independent of energy and seem to be associated with the magnitude of the nuclear density. These ratios display 15–25% enhancement relative to the value of one in the low density limit. Our findings for the σ_T and σ_R super ratios bear qualitative resemblance to the angular distribution ${}^{12}\text{C}/{}^6\text{Li}$ super ratio at 715 MeV/c recently presented [18]. Recent quasifree K^+ scattering data [21] on D, C, Ca, and Pb at $p_L = 705$ MeV/c also suggest enhancement of the K^+ nuclear interaction in the nuclear medium. The present status of K^+ nuclear scattering with due consideration also of older data has been reviewed by Hungerford [22].

Theoretical attempts to explain the apparent strong enhancement of the K^+ nuclear interaction as exhibited in earlier data, and by the present findings, have been mostly limited to the ${}^{12}\text{C}$ data. The nuclear medium effects associated with ‘‘nucleon swelling’’ [5] and with density dependence of the exchanged vector meson masses [6] give rise to a more repulsive K^+ nuclear potential than the (already repulsive) first order $t\rho$ optical potential. However, the density dependence of V_{opt} obtained by fitting to the σ_T and σ_R values derived in the present work is such that V_{opt} now contains, in addition to the low-density repulsive $t\rho$ component, also a higher-density attractive component which largely cancels the $t\rho$ repulsion inside the nucleus. A significant enhancement for σ_T was shown in the most recent work of Ref. [7] to result from the density dependence of the medium NN interaction within a relativistic random-phase approximation K^+ -nucleus calculation. However, this same method when applied [23] to evaluate the longitudinal and transverse response functions for quasielastic electron scattering on ${}^{12}\text{C}$ does not lead to good agreement with the data. It is interesting to note that the effect calculated for ${}^6\text{Li}$ yields σ_T values substantially higher than required, so that if super ratios of the kind presented here in Fig. 3 relative to ${}^6\text{Li}$ were considered by these authors, a significant departure from the value of one would occur, in agreement with our conclusions. Finally, the more conventional nuclear medium effects such as Fermi averaging, three-body kinematics and off-shell KN corrections have been shown in Ref. [5], and more recently in Ref. [8] for all four nuclear targets with published σ_T values, to provide only minor corrections of the order of a few percent to the first-order $t\rho$ optical potential considered in this work as a theoretical benchmark. These corrections are insufficient to resolve the discrepancy with experiment.

Another nuclear medium effect recently proposed [24–26] is due to meson exchange currents (MEC) arising from the interaction of K^+ with the excess pion cloud in ${}^{12}\text{C}$. The

pion production threshold about $p_L \approx 400$ MeV/c generates a strong energy dependence for this effect in the p_L range 488–714 MeV/c of interest here. Such energy dependence is indeed apparent in the ratios $\sigma(\text{expt})/\sigma(\text{calc})$ shown in Fig. 2, but on the other hand the super ratios of Fig. 3 suggest that *nuclear medium* corrections to the K^+ nuclear interaction should be essentially energy independent. We also point out that the MEC mechanism considered in Refs. [25,26] contributes to the calculation of σ_T values mainly through changing (increasing) the imaginary part of V_{opt} , whereas the revised σ_T and new σ_R values require, according to our fits, a substantial energy-dependent (attractive) modification of the real part of V_{opt} . We have checked that increasing the imaginary part of the $t\rho$ optical potential by adding a ρ^2 term, as suggested in Ref. [26], does not resolve the discrep-

ancy between experiment and calculation for the σ_T and σ_R values presently reported, except partly for σ_T in ^{12}C . In conclusion, there seems to remain a significant and puzzling discrepancy between theory and experiment for K^+ nuclear interactions at intermediate energies ($p_L \approx 500$ –800 MeV/c).

ACKNOWLEDGMENTS

This research was supported by the Israel Science Foundation administered by the Israel Academy of Sciences and Humanities, by the U.S.-Israel Binational Science Foundation and by the U.S. Department of Energy (DE-AC02-76CH00016).

-
- [1] Y. Mardor *et al.*, Phys. Rev. Lett. **65**, 2110 (1990).
 [2] R.A. Krauss *et al.*, Phys. Rev. C **46**, 655 (1992).
 [3] R. Sawafta *et al.*, Phys. Lett. B **307**, 293 (1993).
 [4] R. Weiss *et al.*, Phys. Rev. C **49**, 2569 (1994).
 [5] P.B. Siegel, W.B. Kaufmann, and W.R. Gibbs, Phys. Rev. C **30**, 1256 (1984); **31**, 2184 (1985).
 [6] G.E. Brown, C.B. Dover, P.B. Siegel, and W. Weise, Phys. Rev. Lett. **60**, 2723 (1988).
 [7] J.C. Caillon and J. Labarsouque, Phys. Rev. C **45**, 2503 (1992); Phys. Lett. B **295**, 21 (1992); Nucl. Phys. **A572**, 649 (1994); **A589**, 609 (1995); Phys. Rev. C **53**, 1993 (1996).
 [8] C.M. Chen and D.J. Ernst, Phys. Rev. C **45**, 2019 (1992); M.F. Jiang, D.J. Ernst, and C.M. Chen, *ibid.* **51**, 857 (1995).
 [9] J.W. Cronin, R. Cool, and A. Abashian, Phys. Rev. **107**, 1121 (1957).
 [10] B.W. Allardyce *et al.*, Nucl. Phys. **A209**, 1 (1973).
 [11] M. Arima and K. Masutani, Phys. Rev. C **47**, 1325 (1993).
 [12] W.B. Kaufmann and W.R. Gibbs, Phys. Rev. C **40**, 1729 (1989).
 [13] M.L. Goldberger and K.M. Watson, *Collision Theory* (John Wiley, New York, 1964).
 [14] R.A. Arndt and L.D. Roper, Phys. Rev. D **31**, 2230 (1985).
 (SAID on-line program); **46**, 961 (1992).
 [15] C.W. de Jager, H. de Vries, and C. de Vries, At. Data Nucl. Data Tables **14**, 479 (1974); H. de Vries, C.W. de Jager, and C. de Vries, *ibid.* **36**, 495 (1987).
 [16] H.A. Bethe, Phys. Rev. **89**, 1256 (1953); W.T. Scott, Rev. Mod. Phys. **35**, 231 (1963).
 [17] CERN subroutine PHYS325 (unpublished).
 [18] R. Michael *et al.*, Phys. Lett. B **382**, 29 (1996).
 [19] E. Friedman, A. Gal, and C.J. Batty, Phys. Lett. B **308**, 6 (1993); Nucl. Phys. **A579**, 518 (1994).
 [20] O. Meirav *et al.*, Phys. Rev. C **40**, 843 (1989).
 [21] C. Kormanyos *et al.*, Phys. Rev. Lett. **71**, 2571 (1993); Phys. Rev. C **51**, 669 (1995).
 [22] E.V. Hungerford, Nucl. Phys. **A585**, 121c (1995).
 [23] J.C. Caillon and J. Labarsouque, Nucl. Phys. **A595**, 189 (1995).
 [24] S.V. Akulinichev, Phys. Rev. Lett. **68**, 290 (1992).
 [25] M.F. Jiang and D.S. Koltun, Phys. Rev. C **46**, 2462 (1992).
 [26] C. Garcia-Recio, J. Nieves, and E. Oset, Phys. Rev. C **51**, 237 (1995); U.G. Meißner, E. Oset, and A. Pich, Phys. Lett. B **353**, 161 (1995).